Int. J. Solids Structures Vol. 22, No. 7, pp. 677–692, 1986
Printed in Great Britain.

0020–7683/86 $3.00 + .00
Pergamon Journals Ltd.

STUDY OF THE NON-UNIFORM GROWTH OF A PLANE CRACK IN A THREE-DIMENSIONAL BODY SUBJECTED TO NON-PROPORTIONAL LOADINGS

R. BILLARDON, C. ADAM and J. LEMAITRE
Laboratoire de Mécanique et Technologie, E.N.S.E.T./Université Paris 6/C.N.R.S.,
61, Avenue du Président Wilson, 94230 Cachan, France

(*Received* 2 *May* 1985)

Abstract—A rod with a circular section is subjected to a cyclic four-point bending moment so that a crack initiates from a circumferential V-notch and propagates in the plane of symmetry. By rotating the specimen through arbitrary angles from time to time, complicated crack front shapes are obtained. One of these complicated crack fronts, the evolution of which is experimentally observed, is modelled by using three-dimensional boundary elements. Different virtual crack extensions are simulated in which local extensions correspond to the growth of the crack front along only one element side and global extensions correspond to the uniform or non-uniform growth of the whole crack front. In each case, the strain energy release rate is calculated either from its energetic definition or from the values of the stress intensity factors. The calculations confirm the validity of the maximum energy release rate criterion to predict the crack front evolution.

INTRODUCTION

The general problem of the directional criteria for cracks lying in three-dimensional bodies subjected to cyclic or static non-proportional loadings is of prime interest in the case of large shafts, rolling mills, thick pressure vessels....

The restricted case of the bifurcation of a crack in an elastic two-dimensional body has given rise to abundance of literature. Figure 1 illustrates a particular and frequently studied case: as long as the two sets of forces F_1 and F_2 remain equal to each other, the crack lying in the middle of the "infinite" plate grows in the same direction as its original orientation; but, as soon as the ratio of F_1 to F_2 is modified a kink appears. The first directional criteria proposed for such cases refer to the stress field in the vicinity of the crack tip calculated just before the crack deviates from its previous direction:

(i) For Erdogan and Sih[1], the direction of the kink is the direction where the maximum principal stress is maximum just before the bifurcation.

(ii) For Sih[2], the direction of the kink is the direction where the strain energy density has an extremum value just before the bifurcation.

On the contrary, more recently proposed criteria refer to the stress field in the vicinity of the tip of an infinitesimal kink, in other words, calculated just after the crack has deviated from its previous direction:

—For instance, Bilby and Cardew[3] proposed that the direction of the kink is such that the stress intensity factor K_{II}^{*}, calculated after the bifurcation has occurred, is null.

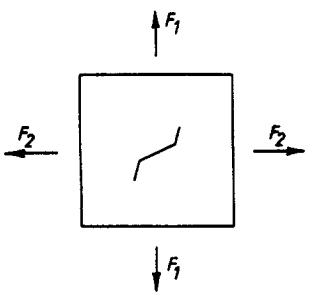

Fig. 1. Bifurcation of a crack in a two-dimensional body.

When applied to various situations by many authors all those criteria resulted in similar, although generally different numerical solutions. But it was only recently that Leblond and Amestoy[4] succeeded in proving the differences obtained are due to nothing but numerical approximations: indeed, within the framework of conventional elasticity, it is now analytically demonstrated that all those criteria are equivalent to the maximization of the energy released in the structure if the surface separation energy 2γ first defined by Griffith[5] is assumed to be a constant. To complete this review, it can be noticed with Boissenot and Dubois[6] that the crack extension force concept introduced by Strifors[7] is also directly deduced from Griffith's theory. Lastly, this point is even more obvious for the path independent integrals J_I and J_{II} introduced by Bui and Proix[8] to separate the stress intensity factors K_I and K_{II} in mixed mode problems.

In the two-dimensional case, the solution to be found is the bifurcation angle of the crack, i.e. a scalar, whereas the unknown of the general three-dimensional problem is a set of vectors, the components of which are the crack velocities all along the crack front. Again, different criteria have been proposed but each of them belongs to one of the following distinct approaches:

(i) So-called "local criteria" involve the fulfilment of a fracture criterion at any point along the front of the crack.

(ii) So-called "global criteria" involve a maximization of the strain energy release rate for the cracked structure taken as a whole.

Only plane cracks subjected to pure mode I in three-dimensional bodies are considered in this paper which consists of three sections:

(i) In the first one, different local and global criteria available in the literature are discussed.

(ii) Then, a new experiment which enables to obtain under non-proportional loadings complicated crack fronts, the evolution of which may be strongly non-uniform, is described.

(iii) Lastly, boundary elements analyses of a typical experimentally observed configuration are presented and discussed.

CASE OF A PLANE CRACK IN PURE MODE I

In this paper, the material behaviour is assumed to be purely linear elastic. If δW is the energy dissipated when a newly created crack surface δS appears during the crack growth process, the strain energy release rate is, by definition

$$G = \lim_{\delta S \to 0} \frac{\delta W}{\delta S}. \tag{1}$$

Considering conventional elasticity, this global quantity can be directly linked to the displacements field at the crack tip. Hence, in the two-dimensional case with pure mode I, if plane strain state is assumed,

$$G = \frac{1-\nu^2}{E} K_I^2 \tag{2}$$

E and ν, being respectively Young's modulus and Poisson's ratio, and K_I being the stress intensity factor.

Figure 2(a) lies in the plane of a plane crack propagating in a three-dimensional body. When subjected to a pure mode I loading, the crack front moves from its original position Γ to the new one Γ'. The cracked surface newly created locally at point M during the crack growth process is

$$\delta S_{|MM'} = a \cdot \lambda(s) \cdot \mathrm{d}s, \tag{3}$$

where s is the curvilinear abscissa along the crack front, and where a and $\lambda(s)$ represent the amplitude and the shape function defining the crack growth, respectively. Of course, the

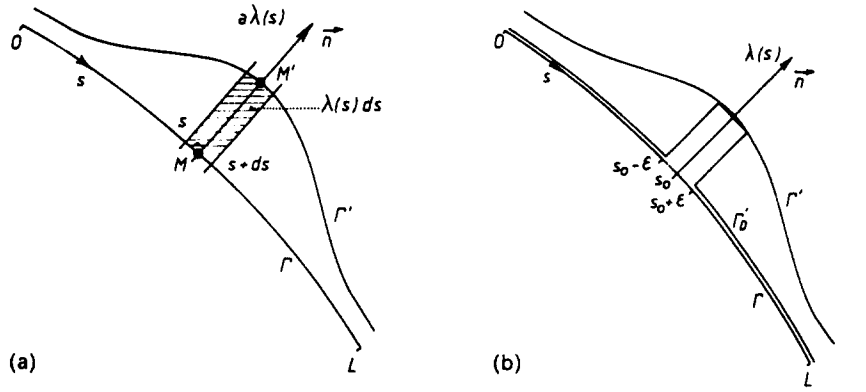

Fig. 2. (a) Crack front of a plane crack in a three-dimensional body. (b) Very local extension.

condition $\delta S \to 0$ of relation (1) corresponds to the condition $a \to 0$. So, a directional criterion deals only with the determination of $\lambda(s)$, the crack growth velocity dependent on the abscissa s along the crack front. In a three-dimensional body, it is proved for plane cracks of arbitrary shape[9], and generally speaking it can be assumed, that plane strain state conditions exist along the crack front. Hence[10], the two-dimensional relation (2) can be extended as

$$G = \lim_{a \to 0} \frac{a \dfrac{1-\nu^2}{E} \displaystyle\int_\Gamma [K_I(s)]^2 \cdot \lambda(s) \cdot ds + 0(\lambda^{3/2})}{a \displaystyle\int_\Gamma \lambda(s) \cdot ds + a^2 \int_\Gamma \frac{[\lambda(s)]^2}{2 \cdot \rho(s)} ds} \,, \tag{4}$$

where $\rho(s)$ is the curvature radius of the crack front.

So, from relation (4), or from a straightforward extension of relations (1) and (2), a value noted G_{K_I} of the strain energy release rate can be calculated from the K_I values according to the relation:

$$G_{K_I} = \frac{1-\nu^2}{E} \frac{\displaystyle\int_\Gamma [K_I(s)]^2 \cdot \lambda(s) \cdot ds}{\displaystyle\int_\Gamma \lambda(s) \cdot ds} \tag{5}$$

Local criteria

The simplest local criterion applying to the case illustrated by Fig. 2(a) consists of the extension of Irwin's criterion:

$$\operatorname*{Sup}_s K_I(s) = K_I(s_0) = K_{I_c} \tag{6}$$

where K_{I_c} is the critical stress intensity factor characteristic of the material toughness. It must be noticed that:

(i) The directional criterion is not disconnected from the fracture criterion itself.

(ii) Such a criterion does not give any indication on $\lambda(s)$ for any abscissa $s \neq s_0$.

At any rate, to become a true directional criterion, such a formulation must be extended by adding a local crack propagation law.

Global criteria

All the global criteria proposed to replace the above-discussed local criteria refer to the maximization of the strain energy release rate in the whole structure. They can be written as follows.

Find λ^* so that

$$G(\lambda^*, F_c) = \text{Sup } G(\lambda, F_c) \tag{7a}$$

with the constraint

$$G(\lambda^*, F_c) = D(\lambda^*). \tag{7b}$$

where $D(\lambda)$ is the dissipation rate and where F_c represents the critical value of the external forces applied to the structure. It can be noticed that, although the fracture criterion is part of the optimization problem (7a, 7b), the solution of this problem may *a priori* lead to any vector $\lambda(s)$.

In the case of the first criterion of this kind which was proposed by Lemaitre[11, 12], it is assumed that the dissipation refers to a constant surface separation energy 2γ. Hence, the optimization problem (7a, 7b) is completely defined after the addition of:

$$D(\lambda) = 2\gamma \int_\Gamma \lambda(s) \cdot \mathrm{d}s \tag{8a}$$

with

$$\int_\Gamma \lambda(s) \cdot \mathrm{d}s = 1 \tag{9a}$$

Labourdette and co-workers[13, 14], considered the same expression of the dissipation rate as in relation (8a), but proposed another strategy for the maximization of the energy released during the crack growth process so that relation (9a) is replaced by

$$\int_\Gamma [\lambda(s)]^2 \cdot \mathrm{d}s = 1. \tag{9b}$$

On the contrary, Bui and Dang Van[15] altered Lemaitre's formulation in keeping relation (9a) but in adding to the surface separation energy a "line energy" and a "curvature energy" corresponding to the variations respectively of the length and of the curvature of the crack front. So, relation (8a) is replaced by

$$D(\lambda) = \int_\Gamma \left\{ 2\gamma \cdot \lambda(s) + \alpha \frac{\lambda(s)}{\rho(s)} + \beta \left[\frac{\lambda(s)}{[\rho(s)]^2} + \lambda''(s) \right] \right\} \tag{8b}$$

where α and β are material dependent parameters.

As Bui and Dang Van's parameters α and β have never been experimentally identified and as Labourdette's criterion introduces no real new physical concept, the criterion used in this study is Lemaitre's "maximum strain energy release rate criterion" described by relations (7a, 7b, 8a, 9a).

Case of a very local extension

If the stress intensity factor K_I is maximum at the point of abscissa s_0

$$K_I(s_0) \geqslant K_I(s) \qquad \forall s \neq s_0 \tag{10}$$

and if a crack extension Γ'_D localized at this point is considered (see Fig. 2b) according to

relation (5), the following expression holds:

$$G_{K_I|\Gamma'_D} = \frac{\dfrac{1-\nu^2}{E}\displaystyle\int_I [K_I(s_0)]^2 \cdot \lambda(s) \cdot \mathrm{d}s}{\displaystyle\int_I \lambda(s) \cdot \mathrm{d}s} = \frac{C}{D}, \tag{11}$$

where the domain I is defined by

$$\mathrm{I} \equiv \{\lambda(s) = 1,\ [s_0-\varepsilon, s_0+\varepsilon]\}, \tag{12}$$

ε being infinitesimal.

Still according to relation (5), any other crack extension Γ' leads to

$$G_{K_I|\Gamma'} = \frac{\dfrac{1-\nu^2}{E}\displaystyle\int_{\bar{\mathrm{I}}} [K_I(s)]^2 \cdot \lambda(s) \cdot \mathrm{d}s + \dfrac{1-\nu^2}{E}\int_I [K_I(s_0)]^2 \cdot \lambda(s) \cdot \mathrm{d}s}{\displaystyle\int_{\bar{\mathrm{I}}} \lambda(s) \cdot \mathrm{d}s + \int_I \lambda(s) \cdot \mathrm{d}s} = \frac{A+C}{B+D} \tag{13}$$

where the domain $\bar{\mathrm{I}}$ is defined by

$$\bar{\mathrm{I}} \equiv \{\lambda(s) \leqslant 1,\ [0, s_0-\varepsilon[U]s_0+\varepsilon, L]\}. \tag{14}$$

As all the terms A, B, C and D of expressions (11) and (13) are positive and as

$$\frac{C}{D} \geqslant \frac{A}{B} \tag{15}$$

because of assumption (10), it is obvious that

$$G_{K_I|\Gamma'_D} \geqslant G_{K_I|\Gamma'} \qquad \forall \Gamma'. \tag{16}$$

To conclude, the previous calculations prove that the strain energy release rate criterion leads to a non-physically admissible crack extension, localized at the point where the stress intensity factor is maximum. In other words, the global criterion (7a, 7b, 8a, 9a) is strictly equivalent to the local criterion (6). This troublesome conclusion which has already been demonstrated in two different ways by d'Escatha and Labbens[10] and by Nguyen Quoc Son[16], can be argued away as follows: the onset of the crack growth does correspond to a very local extension but, as it is undoubtedly unstable, it leads to subsequent crack growth until a stable and more regular shape of the crack front is reached.

Although the validity of relation (5) cannot be questioned in the case of plane cracks in pure mode I, in the study presented in this paper the value G_{K_I} is compared to the value of the strain energy release rate derived from its energetic definition (1) that is

$$G = \frac{\partial W}{\partial S} = -\frac{\partial W_\varepsilon - \partial W_F}{\partial S} \simeq \frac{W_\varepsilon(\Gamma') - W_\varepsilon(\Gamma)}{\Delta S}, \tag{17}$$

where $W_F(\Gamma)$ and $W_F(\Gamma')$ are the external force energies and $W_\varepsilon(\Gamma)$ and $W_\varepsilon(\Gamma')$ the strain energies corresponding to the same external displacements applied to the structure with respectively the crack front Γ and the subsequent one Γ', the crack surface increase ΔS between Γ and Γ' being incremental.

EXPERIMENTAL PROCEDURE

For this study a new experimental scheme described on Fig. 3 has been designed. The three-dimensional body considered is a rod (component 1) made of 2024 aluminium alloy, 906 mm long and with a circular section 80 mm in diameter. It is subjected to 4-point bending by a displacement controlled hydraulic actuator (component 2). A circumferential 60° V-notch is machined all around the specimen reducing the diameter of the section in the plane of symmetry to 72 mm. As the load applied varies cyclically at a frequency of 1 or 2 Hz from a zero value to a negative value, a crack initiates from the notch and, remaining always open, propagates in the plane of symmetry. The maximum absolute value of the load is equal to 120 kN until the initiation of the crack occurs, and is progressively decreased during the propagation in order to continuously fulfil the small scale yielding assumption.

Three different techniques are used to follow the crack growth:

(i) The electrical potential drop technique involves 12 probes equally distributed all around the specimen. The crack remaining always open, the random noise can be eliminated by the means of a computer averaging 10 successive measurements not to be synchronized with the load. Furthermore, spurious effects such as room temperature variations are eliminated by using as a reference the tension measured simultaneously on an uncracked specimen lying on the same test-bench as the experiment.

(ii) Underloads, the amplitude of which is equal to 50% of the maximum load currently applied, induce for a few cycles a different type of rupture which clearly marks the crack front without modifying its shape.

(iii) Injection of ink can also colour from time to time the cracked surfaces.

Figure 4 shows the evolution of the crack front through one of the specimens tested. The Y axis coincides with the axis of the applied load, and the hatched zone at the bottom of the figure is the ultimate failure zone corresponding to a number of cycles for failure $N_F = 15 \times 10^3$ cycles. At a frequency of 1 Hz, 1470 cycles were necessary to shift from the marked crack front Γ to the next one Γ'. Strain gauge measurements indicate that the spurious torsion moment applied to the specimen is less than 1% of the bending moment and the slight deviation of the initiation from the Y axis can be soundly neglected.

After the crack has reached a certain depth, say at crack front Γ' of Fig. 4, the cycling of the load can be stopped, the specimen is rotated through an arbitrary angle, say 90° clockwise, and then, the cycling of the load is resumed. The dashed lines of Fig. 5 correspond to the crack fronts following this rotation of the specimen. By this means, it can be noticed

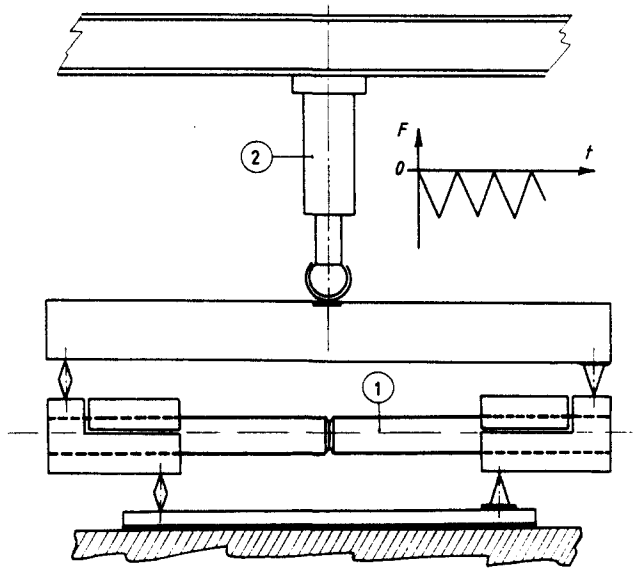

Fig. 3. Experimental scheme.

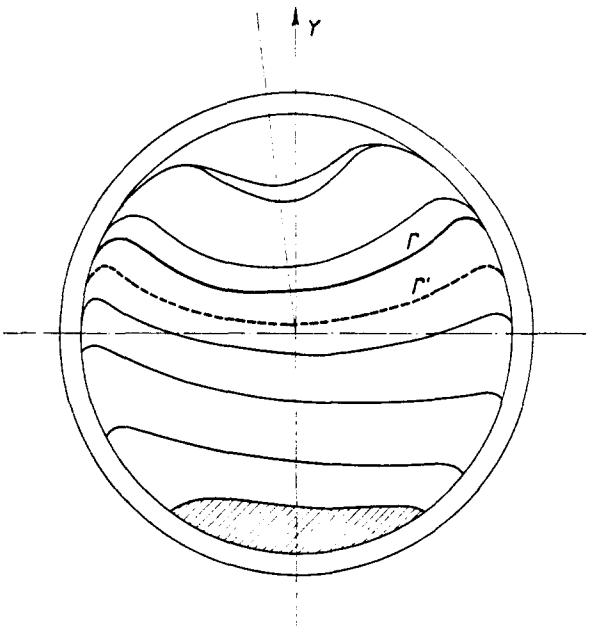

Fig. 4. Evolution of the crack front without rotation of the specimen.

that largely non-uniform crack growths are easily obtained, the crack remaining in its plane and being always subjected to pure mode I as this plane is a plane of symmetry all the time for the whole scheme.

The case chosen for the numerical analysis because of its complexity corresponds to the crack front Γ of Fig. 6. The crack fronts noted Γ_1, Γ_2 and Γ_3 correspond to previous rotations of the specimen respectively through 15° anticlockwise, 30° clockwise, and 60° clockwise.

NUMERICAL ANALYSIS

To avoid too costly finite element calculations the boundary element method is chosen to make this three-dimensional analysis. Using the code CASTOR-3D developed by the

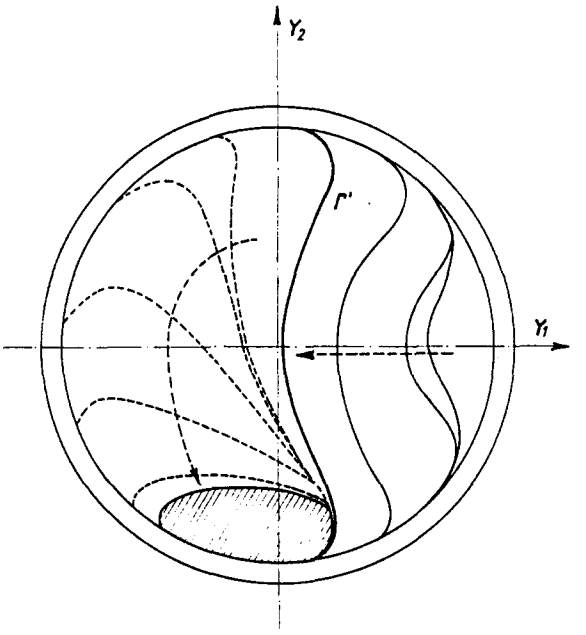

Fig. 5. 90° clockwise rotation of the specimen.

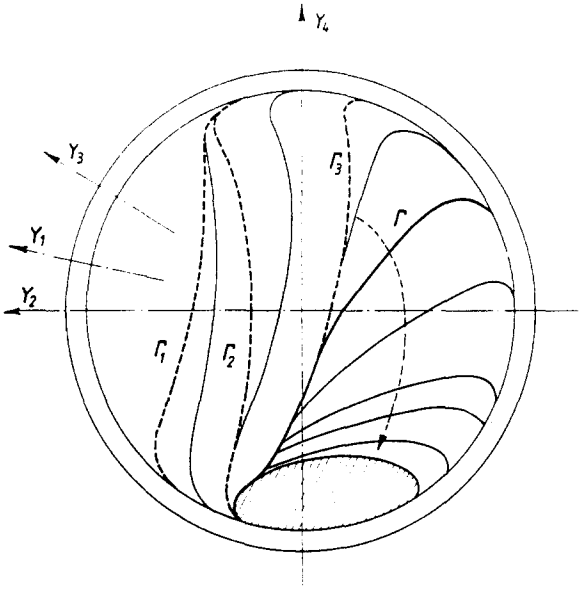

Fig. 6. Analysed case.

French "Centre d'Etudes Techniques des Industries Mécaniques"[17], and taking into account the symmetry, half of the specimen is modelled by 147 conventional 8- or 6-node elements. A view of the mesh (402 nodes with 3 degrees of freedom per node) is given in Fig. 7(a). At the free end of the specimen the load applied is modelled through fixed displacements so that

$$U_z = \alpha \cdot Y, \tag{18}$$

where α is a constant factor proportional to the load amplitude. A more detailed view of the mesh in the plane of the crack is given in Fig. 7(b). In Fig. 7(a), the shaded zone corresponds to a prescribed null displacements zone taking into account a partial closure of the crack.

Calculations of the stress intensity factors

The directions numbered from Π_1 to Π_{11} on Fig. 7(b) correspond to the intersection, with the plane of the crack, of planes normal to both the plane of the crack and the crack front. They also correspond to the boundaries between the quadrilateral elements along the crack front, or to the lines joining the middle side nodes of the same elements as indicated on Fig. 8(a). The distance counted from the crack front along those directions is noted r. If w is the displacement U_z, i.e. half the crack opening, the stress intensity factor can be calculated as

$$K_1 = \frac{\sqrt{2\pi}}{4} \frac{E}{1-\nu^2} \cdot \lim_{r \to 0} \frac{w}{\sqrt{r}} \tag{19}$$

assuming as before [see relation (4)] a plane strain state all along the crack front. Neither special nor distorted (also called quarter-point) elements[18] are used at the crack tip to model the stress singularity. Besides, as there are no more than one or two lines of elements with a constant width behind the crack front, the simple extrapolation technique illustrated by Fig. 8(b) is adopted. Of course, the K_1 values obtained by this means suffer from a lack of accuracy which may amount to about 2–8%, according to calculations made by various authors in two- or three-dimensional conditions with finite or boundary elements [18–20].

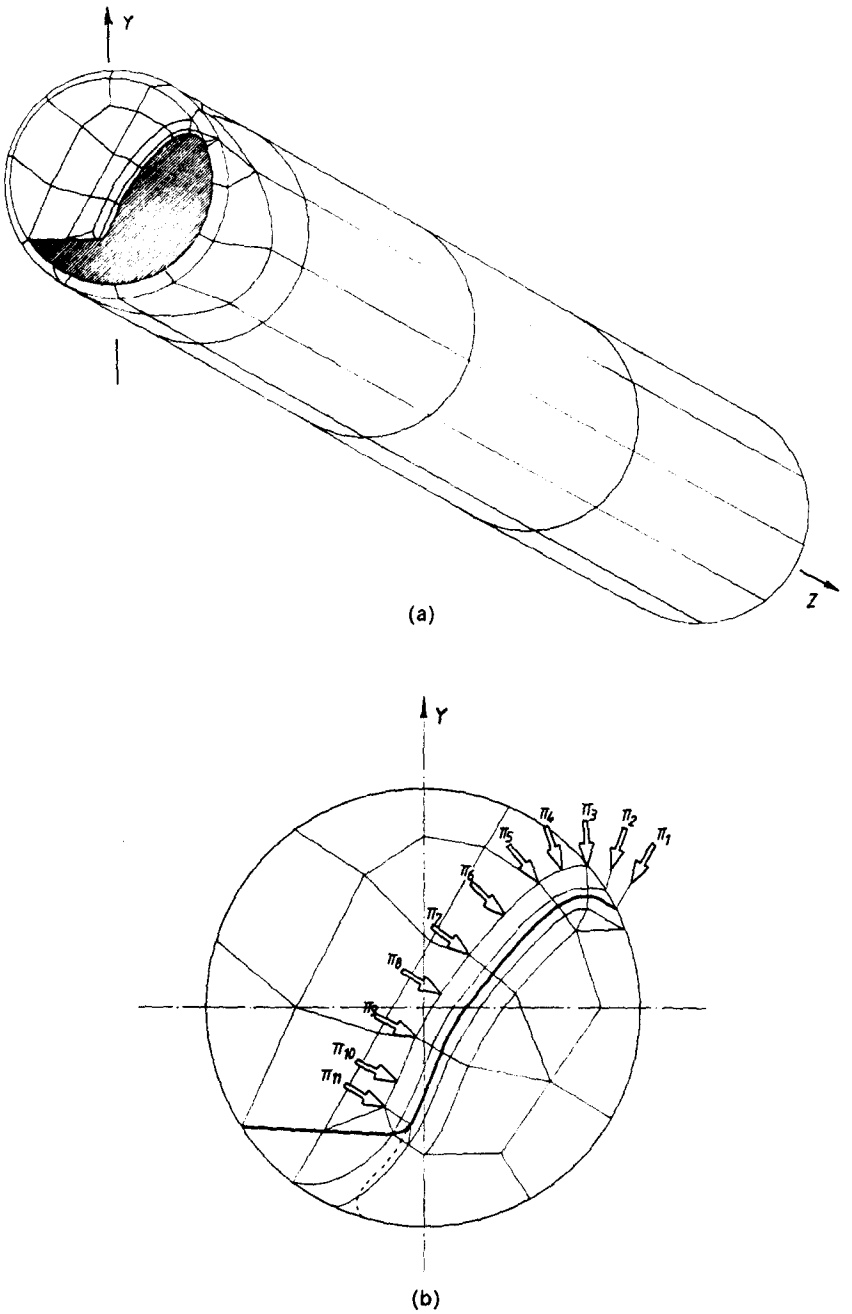

Fig. 7. (a) Boundary elements mesh. (b) Mesh in the plane of the crack.

Local and global extensions of the crack

To numerically model a crack extension localized at one point of the crack front, the boundary of the corresponding element along the crack front is distorted as indicated in Fig. 9(a). The middle side node is displaced by $\lambda_i = \frac{1}{3}$ mm. This quantity is chosen large enough to induce significant numerical results and small enough to be considered as "incremental". Of course, because of the shape functions of the 8-node elements, such local extensions are parabolic. But configurations obtained by shifting a corner node instead of a middle side node as indicated in Fig. 9(b) are non-admissible. Hence, only local extensions in the directions Π_2, Π_4, Π_6, Π_8 and Π_{10} of Fig. 7(b) are considered. An example of the extension localized in the direction Π_4 is illustrated by Fig. 10, the displacement λ_4 being magnified by a factor of 5.

Figure 11 illustrates an almost uniform global extension for which $\lambda_i = \frac{1}{3}$ mm for all i

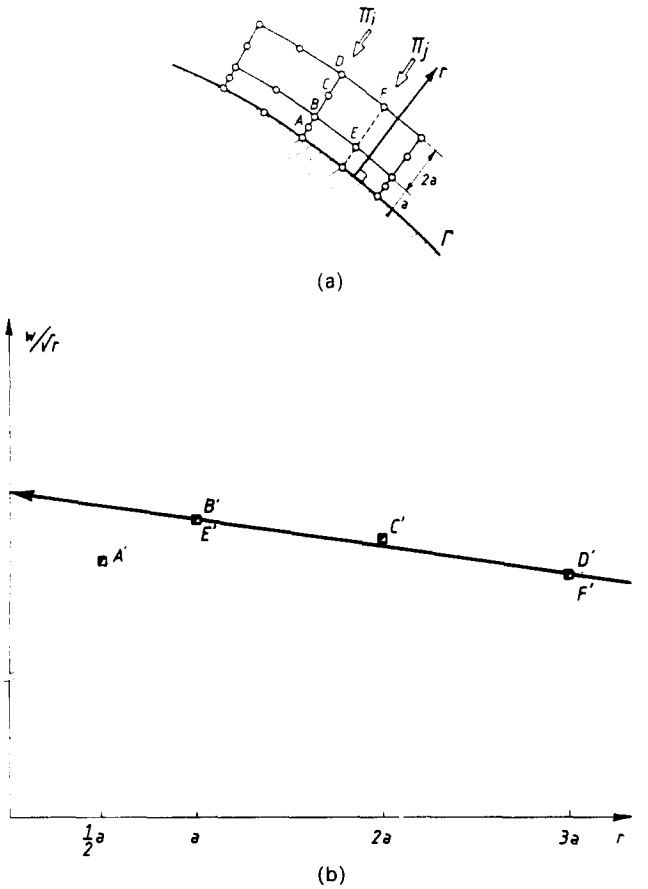

Fig. 8. (a, b) Determination of the stress intensity factors.

from 2 to 11. Figures 12 and 13 illustrate non-uniform global extensions for which the maximum extension is equal to $\frac{1}{3}$ mm. For all those figures the displacements are also magnified by a factor of 5. Figure 13 corresponds to the experimentally observed crack growth.

Calculations of the strain energy release rate

To summarize, nine different three-dimensional analyses of the specimen are performed considering different crack fronts and the same loading:

(i) The first analysis corresponds to the initial crack front Γ of Fig. 7(b). The outcomes of this analysis are the stress field in the vicinity of the crack tip along the crack front, the

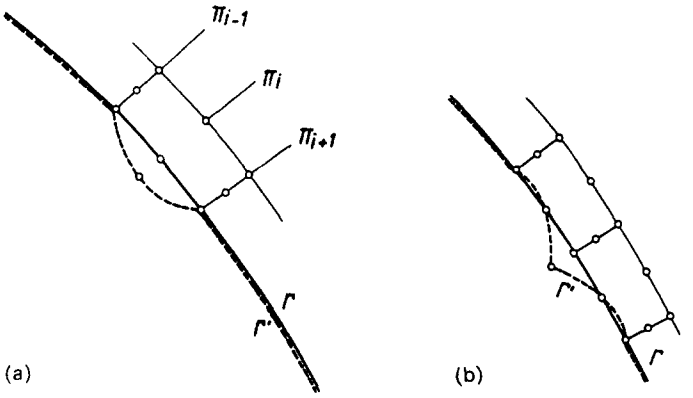

Fig. 9. (a, b) Admissible and non-admissible local extensions.

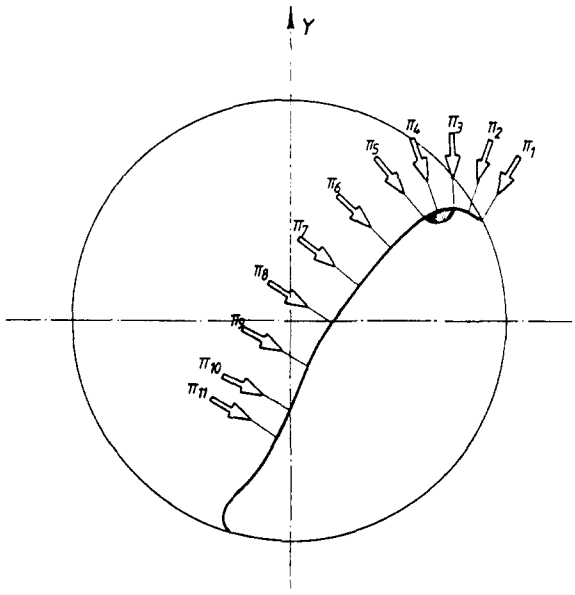

Fig. 10. Local extension in the direction π_4.

strain energy $W_\varepsilon(\Gamma)$ [cf. relation (17)] and the stress intensity factors estimated in the directions Π_1 to Π_{11} according to relation (19).

(ii) Five analyses correspond to the crack front Γ "incrementally" distorted locally in the directions Π_2, Π_4, Π_6, Π_8 and Π_{10}. The last three analyses correspond to the uniform and non-uniform "incremental" growths depicted by Figs. 11–13. In each case the strain energy $W_\varepsilon(\Gamma')$ is calculated.

After the calculation of the crack surface increases

$$\Delta S = \int_\Gamma \lambda(s) \cdot \mathrm{d}s \tag{20}$$

bounded by the piecewise parabolic crack fronts Γ and Γ', the strain energy release rates G corresponding to the eight local or global extensions considered are easily derived from the relation (17).

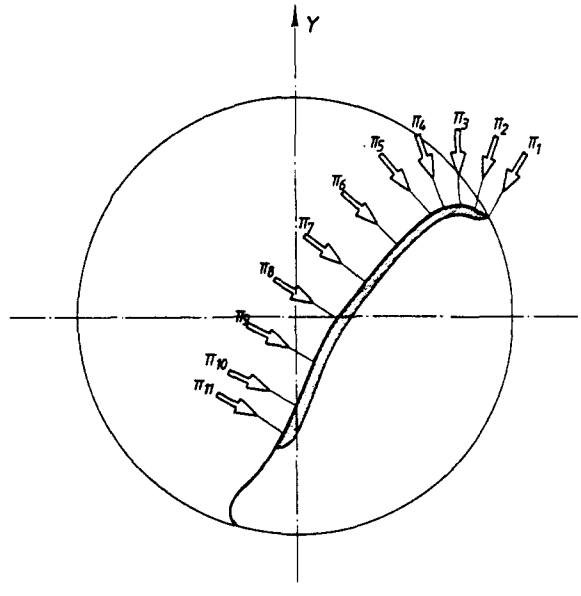

Fig. 11. Uniform global extension.

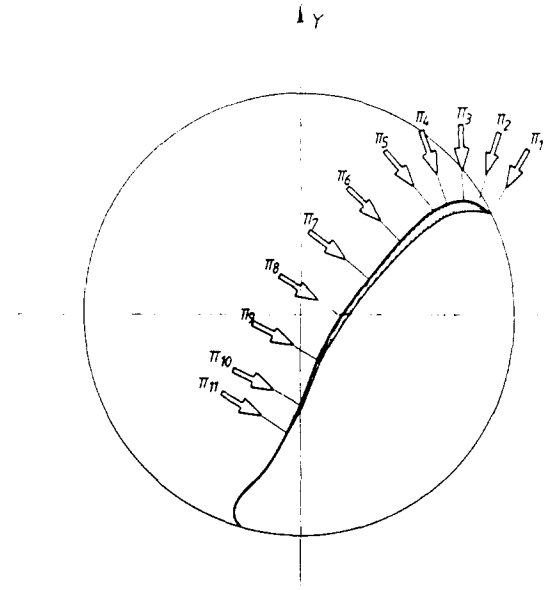

Fig. 12. Non-real non-uniform global extension.

To evaluate the G_{K_1} values corresponding to the eight local or global extensions considered extra calculations are required. The numerator of relation (5) is numerically calculated as

$$\Delta W = \frac{1-\nu^2}{E} \sum_i \int_{\delta\Gamma_i} [K_I(s)]^2 \cdot \lambda(s) \cdot ds \tag{21}$$

where $\delta\Gamma_i$ is the part of the crack front Γ corresponding to element i. Noting K_{I_n} and λ_n the known values of K_I and λ at node n of element i, and assuming the same parabolic variation for both quantities, a geometrical transform leads to the relations

$$\lambda(\xi) = \sum_{n=1}^{3} N_n(\xi) \cdot \lambda_n \tag{22a}$$

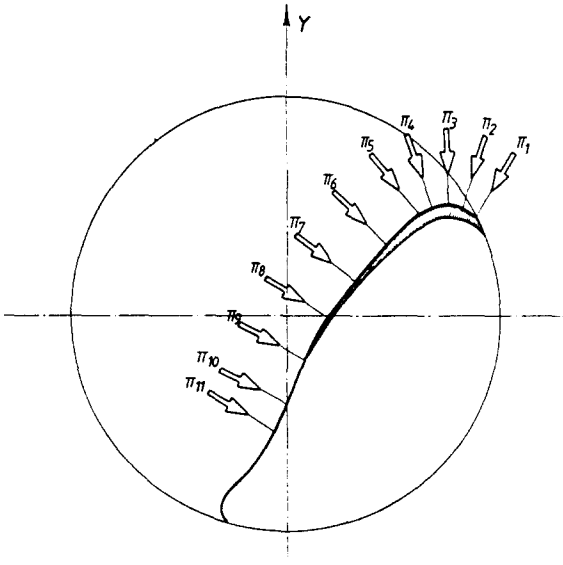

Fig. 13. Real non-uniform global extension.

$$K_I(\xi) = \sum_{n=1}^{3} N_n(\xi) \cdot K_{I_n} \tag{22b}$$

where $N_n(\xi)$ are the usual shape functions with $\xi = -1, 0$ and $+1$ respectively for $n = 1, 2$ and 3. So, expression (21) becomes

$$\Delta W = \frac{1-\nu^2}{E} \sum_i L_i \left[\int_{-1}^{+1} [K_I(\xi)]^2 \cdot \lambda(\xi) \cdot d\xi \right] \tag{23}$$

or

$$\Delta W = \frac{1-\nu^2}{E} \sum_i L_i \left[\int_{-1}^{+1} f(\xi) \cdot d\xi \right] \tag{24}$$

where L_i is the length of $\delta\Gamma_i$.

Finally, a 5-Gauss point integration rule leads to

$$\Delta W = \frac{1-\nu^2}{E} \sum_i \left[\sum_{N=1}^{5} w_N \cdot f(\xi_N) \right] \tag{25}$$

with w_N and ξ_N being respectively the weight function and the coordinate of Gauss point N.

NUMERICAL RESULTS AND DISCUSSION

Local extensions of the crack

Table 1 summarizes the results obtained for the calculations of K_I along the original crack front Γ and for the calculations of G_{K_I} and G corresponding to the five local extensions considered. The K_I values given are percentages of the maximum value of K_I obtained for the direction Π_5. The G_{K_I} and G values given are percentages of the maximum values respectively of G_{K_I} and G obtained for the global uniform extension (cf. Fig. 11).

First, it can be noticed that the new experimental procedure developed for this study is an easy means of obtaining complicated crack fronts subjected to pure mode I along which the stress intensity factor K_I can vary in large proportions: for the studied crack front Γ, the range of the K_I values calculated exhibits a ratio of maximum to minimum values greater than 10.

As it is recalled that no local extension could be considered in the direction Π_5, it can be concluded that, as expected, the local extension which maximizes the strain energy release rate, whatever its evaluation G or G_{K_I}, is the extension localized at the point where K_I is maximum.

Table 1

Direction	K_I (%)	G_{K_I} (%)	G (%)	$\left\|\frac{\log a}{\log G_{K_I}}\right\|$
π_1	59.5			
π_2	76.0	142.4	113.7	
π_3	92.0			
π_4	99.5	239.4	148.6	1.50
π_5	100.0			
π_6	79.0	156.2	98.8	1.48
π_7	60.5			
π_8	46.0	52.1	35.1	1.50
π_9	28.0			
π_{10}	7.5	1.7	—	$\simeq 1.7$
π_{11}	$\simeq 0$			

Table 2

Extension	Uniform global Fig. 11	Non-uniform global Fig. 12	Non-uniform global Fig. 13
G_{K_1} (%)	100.0	140.9	160.9
G (%)	100.0	139.5	155.3

Global extensions of the crack

Table 2 summarizes the results obtained for the global uniform extension (cf. Fig. 11) and the global non-uniform extensions corresponding to Figs. 12 and 13. The G_{K_1} and G values are normalized in the same way as in Table 1.

Of course, since only two global non-uniform extensions are considered, no final conclusion can be formulated. However, it is remarkable that the global (physically admissible) extension which maximizes the strain energy release rate whatever its evaluation G or G_{K_1}, is the non-uniform global growth observed experimentally and illustrated by Fig. 13.

Comparison of the G_{K_1} values with the G values

A weighted value of G_{K_1} can be calculated as follows

$$\overline{G_{K_1}} = \frac{\sum_i (G_{K_1})_i \cdot L_i}{\sum_i L_i} = 96.8 \tag{26}$$

where L_i is the length of the part of the crack front which belongs to element i, and $(G_{K_1})_i$ the value of G_{K_1} calculated for the local crack extension corresponding to the same element i. Of course, the summations are extended to the whole crack front so that the denominator of expression (26) is equal to the total length of Γ. The numerical value obtained (96.8) is to be compared to the value of G_{K_1} corresponding to the global uniform crack extension (100.0). Considering the accuracy of all the numerical calculations and especially of the determination of the stress intensity factors, the similarity of the two values, which should be equal, proves the quality of the G_{K_1} values calculations.

The weighted value of G, $\bar{G} = 63$, is obtained in the same way. On the contrary this value, far from the value 100, proves that the coarse mesh used for the calculations involving "smooth" crack fronts (like Γ or Γ' for global extensions) is not suitable any more. It is comparatively too stiff for crack fronts strongly distorted by very local extensions. In those cases, finer and hence less stiff meshes in the vicinity of the crack front should have been used and larger and more accurate values of G would have been obtained.

The above-mentioned criticism does not hold for the determination of G in the case of global uniform or non-uniform crack extensions. This point is confirmed by the similarity of the respective variations of G and G_{K_1} for different global crack extensions as outlined by Table 2.

Local crack propagation law

To predict fatigue crack propagation the most standard model used is the so-called modified Paris' law [21]. To identify the two material dependent parameters of this model independently of the stress state considered (cf. [22]) it must be written as

$$\frac{dS}{dN} = L \cdot f(G_M^{1/2} - G_{Th}^{1/2}), \tag{27}$$

where dS/dN is the created cracked surface per cycle, and f a power function of the strain

energy release rates G_M and G_{Th} corresponding respectively to the maximum and the threshold loads applied during one cycle. L stands for the total length of the crack front: for instance

$$L = t, \tag{28a}$$

if t is the thickness of a thin plate with a through-crack, or

$$L = 2\pi R, \tag{28b}$$

if R is the front radius of a circumferential crack growing radially in a cylindrical specimen.

In the general three-dimensional case, the "global" expression (27) can be applied "locally" at each point of abscissa s of the crack front if written as:

$$\frac{d}{dN}(a|_s \cdot \delta L) = \delta L \cdot f[(G_M^{1/2} - G_{Th}^{1/2})|_s], \tag{29}$$

where δL is an infinitesimal length of the crack front in the vicinity of the point considered, and $a|_s$ the crack growth per cycle measured normally to the crack front at the same point. Hence,

$$\frac{d}{dN}(a|_s) = f[(G_M^{1/2} - G_{Th}^{1/2})|_s], \tag{30}$$

where $(G_M^{1/2} - G_{Th}^{1/2})|_s$ refers to the strain energy release rates corresponding to extensions localized at the point of abscissa s.

During the experiment, a crack front subsequent to crack front Γ was marked in order to enable an approximate measurement of $(d/dN)(a|_s)$ along Γ. Because of the quick evolution of the strong curvature of the crack front in this region the measurements in the planes Π_1, Π_2 and Π_3 are considered non-reliable. Besides, the accuracy of the measurement made in the plane Π_{10} is quite poor because of the small crack growth. As the loading is applied so that the crack remains always open,

$$(G_M^{1/2} - G_{Th}^{1/2})|_s = G^{1/2}|_s = G_{K_1}^{1/2}|_s. \tag{31}$$

The values of the norm of the ratio $\log a/\log G_{K_1}$ given in Table 1 are obtained from the measurement of the crack growth $a(s)$ in the planes Π_4, Π_6, Π_8 and Π_{10}, and from the calculation of G_{K_1} for the corresponding local extensions. Although few points are considered, the almost constant value obtained despite a wide range of stress intensity factors tends to prove the validity of the local crack propagation law (30).

CONCLUSIONS

A new experimental procedure has been developed to obtain plane cracks subjected to pure mode I and exhibiting a large range of stress intensity factors along complicated crack fronts.

Although no general conclusion can be deduced from a sole numerical calculation, in an arbitrary chosen case boundary elements analyses give rise to the following results:

(i) The local extension which maximizes the strain energy release rate is the extension localized at the point where the stress intensity factor is maximum.

(ii) The value of the strain energy release rate corresponding to a uniform global extension is the weighted value of the strain energy release rate corresponding to local extensions considered all along the crack front.

(iii) If only physically admissible crack extensions are considered, viz. if very local extensions are excluded from the maximization procedure, the extension which maximizes

the strain energy release rate is the non-uniform global growth observed experimentally.

(iv) The crack growth rate at each point of the crack front can be modelled through a local fatigue crack propagation law.

REFERENCES

1. F. Erdogan and G. C. Sih. On the crack extension in plate under plane loading and transverse shear. *J. Basic Engng* 519–527 (1963).
2. G. C. Sih, Strain energy density factor applied to mixed mode crack problems. Institute of Fracture and Solid Mechanics, Technical Report, Lehigh University (1972).
3. B. A. Bilby and G. E. Cardew, The crack with a kinked tip. *Int. J. Fracture* **11,** 708–712 (1975).
4. J. B. Leblond and M. Amestoy, Sur l'universalité de la relation liant les facteurs d'intensité de contraintes d'une fissure juste avant et juste après un changement de direction. *C.R. Acad Sci., Paris* (II) **300,** 643–646 (1985).
5. A. A. Griffith, The phenomenon of rupture and flow in solids. *Phil. Trans. R. Soc., Lond.* **A,** 221 (1920).
6. J. M. Boissenot and M. Dubois, Study of directional criteria of crack instability. *J. Méc. Appliquée* **1,** 133–157 (1977).
7. H. C. Strifors, A generalized force measure of conditions at crack tips. *Int. J. Solids Structures* **10,** 1389–1404 (1974).
8. H. D. Bui and J. M. Proix, Numerical analysis of stress intensity factors in mixed mode problems by path independent integrals J_1 and J_{II}. *Proc. 3rd Int. Conf. Numerical Methods in Fracture Mechanics*. Pineridge Press, Swansea (1984).
9. H. D. Bui, An integral equations method for solving the problem of a plane crack of arbitrary shape. *J. Mech. Phys. Solids* **25,** 29–39 (1977).
10. Y. d'Escatha and R. Labbens, Remarques sur deux critères de rupture fragile pour les problèmes tridimensionnels en mode I. *J. Méc. Appliquée* **2,** 541–552 (1978).
11. J. Lemaitre, Extension de la notion de taux d'énergie de fissuration aux problèmes tridimensionnels et non linéaires. *C.R. Acad. Sci., Paris* (*B*) **282,** 157–160 (1976).
12. J. Lemaitre, Prévision de la croissance des fissures de fatigue dans les structures. *La Fatigue des Matériaux et des Structures*, Editions Maloine (1980).
13. R. Labourdette and J. Pellas, A new approach to the three-dimensional crack growth problem. *Int. J. Fracture* **14,** R121–R124 (1978).
14. R. Labourdette and G. Baudin, An energy approach to the three-dimensional crack growth problem. *Adv. Frac. Res.* **4,** 1859–1869 (1981).
15. H. D. Bui and K. Dang Van, Généralisation de la théorie de la rupture de Griffith. *J. Méc. Appliquée* **3,** 205–225 (1979).
16. Nguyen Quoc Son, Sur l'utilisation des critères de l'énergie en rupture et en fatigue. *C.R. Acad. Sci., Paris* (*A*) **286,** 483–486 (1978).
17. J. C. Lachat and J. O. Watson, Effective numerical treatment of boundary integral equations: a formulation for three-dimensional elastostatics. *Int. J. Num. Meth. Engng* **10,** 991–1005 (1976).
18. R. D. Henshell and K. G. Shaw, Crack tip finite elements are unnecessary. *Int. J. Num. Meth. Engng* **9,** 495–507 (1975).
19. S. S. Palusamy and J. Heliot, Two stress intensity factor calculation methods and solutions for various three-dimensional problems. *Adv. Frac. Res.* **1,** 131–139 (1981).
20. J. M. Boissenot, Analyse tridimensionnelle de la propagation en fatigue d'un défaut de forme semi-elliptique. *Reliability Problems of Reactor Pressure Components*, IAEA-SM 218/43, pp. 33–48. International Atomic Energy Agency Colloquium, Vienna (1978).
21. J. Lemaitre and J. L. Chaboche, *Mécanique des Matériaux Solides*, Chapitre VIII. Editions Dunod (1985).
22. J. M. Virely, Effet d'une surcharge sur la propagation d'une fissure de fatigue dans une structure axisymétrique. *Thèse de 3ème Cycle*, Université Paris 6 (1982).